



Methods to measure, model and manipulate fluid flow in brain

Krishnashis Chatterjee¹, Cora M. Carman-Esparza¹, Jennifer M. Munson^{1,*}

Virginia Tech-Wake Forest School of Biomedical Engineering and Sciences, Department of Biomedical Engineering and Mechanics, Virginia Polytechnic Institute and State University, Blacksburg, VA, United States

ARTICLE INFO

Keywords:

Glymphatic
Lymphatics
Interstitial flow
Cerebrospinal fluid
Computational modeling
In vitro models
MRI

ABSTRACT

The brain consists of a complex network of cells and matrix that is cushioned and nourished by multiple types of fluids: cerebrospinal fluid, blood, and interstitial fluid. The movement of these fluids through the tissues has recently gained more attention due to implications in Alzheimer's Disease and glioblastoma. Therefore, methods to study these fluid flows are necessary and timely for the current study of neuroscience. Imaging modalities such as magnetic resonance imaging have been used clinically and pre-clinically to image flows in healthy and diseased brains. These measurements have been used to both parameterize and validate models of fluid flow both computational and *in vitro*. Both of these models can elucidate the changes to fluid flow that occur during disease and can assist in linking the compartments of fluid flow with one another, a difficult challenge experimentally. *In vitro* models, though in limited use with fluid flow, allow the examination of cellular responses to physiological flow. To determine causation, *in vivo* methods have been developed to manipulate flow, including both physical and pharmacological manipulations, at each point of fluid movement of origination resulting in exciting findings in the preclinical setting. With new targets, such as the brain-draining lymphatics and glymphatic system, fluid flow and tissue drainage within the brain is an exciting and growing research area. In this review, we discuss the methods that currently exist to examine and test hypotheses related to fluid flow in the brain as we attempt to determine its impact on neural function.

1. Introduction

The brain is a complex organ that relies on a carefully controlled environment to function properly. Three different types of fluid are integral to the maintenance of homeostasis as they flow within and around the brain parenchyma. These are the cerebrospinal fluid (CSF), which originates primarily in the choroid plexus and flows through the brain ventricles and into the spinal canal, the cerebral blood (CB or CBF), which is mainly present inside the intracranial arteries and veins, and the interstitial fluid (ISF) which occupies the extracellular space bathing the neuron and glial cells (Fig. 1, Table 1). These fluids deliver nutrients to the brain cells, exchange ions and other substances, remove waste products and provide protective cushioning. Thus, they play important roles in maintaining the proper functioning and the balance of the brain with slight disruptions in the physical or chemical properties of the fluid within the brain can lead to severe abnormalities impairing normal function. Specifically, the movement of the fluid through the compartments of the brain is integral to normal development and function. There have been a number of studies that have identified abnormalities in fluid flow in disease. In order to better

understand how fluid functions and changes within the brain flow, the field has developed a number of advanced measurement techniques and modeling using both computational fluid dynamics and *in vitro* micro-fluidic models. Moving forward, methods to invasively or non-invasively manipulate fluids and flow are required to test causation and remediation of disease phenotypes. The present review article intends to shed light on the importance of fluid flow in the brain by highlighting the recent studies conducted to explore fluid flow within the brain.

2. Measuring fluid flow in the brain

Measurement of fluid in the brain has diagnostic, experimental, and potentially therapeutic planning purposes. There are multiple methods to look at fluid flow in the brain that vary based on fluid flow rates, experimental purpose, availability, and location. Common measurement tools include MRI, Intravital microscopy, Nuclear Medicine (i.e. PET, SPECT, Autoradiography), and Transcranial Doppler. The selection of the type of modality and the usefulness of the measurement is dependent on the question at hand and the purpose of the measurement (i.e. diagnostic vs experimental). The purpose of this section is to

* Corresponding author at: Department of Biomedical Engineering & Mechanics, Kelly Hall 349, 325 Stanger Street, Blacksburg, VA, 24061, United States.
E-mail address: jm4kt@vt.edu (J.M. Munson).

¹ These authors contributed equally to this work.

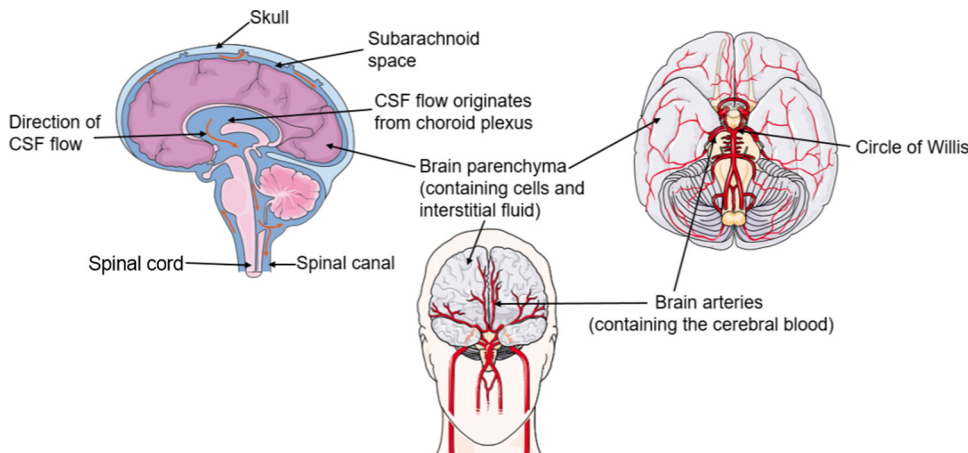


Fig. 1. Location and flow paths of the three main types of fluid flow in brain: cerebrospinal fluid (CSF), interstitial fluid (ISF) and cerebral blood (CB). The CSF originates from the choroid plexus and then flows through the subarachnoid space before draining into the spinal canal, the ISF mainly resides between and around the cells in brain parenchyma and the cerebral blood is mainly present in the intracranial arteries and veins.

Table 1
Physiological and biophysical characteristics of fluids in the brain.

	Cerebrospinal Fluid	Cerebral Blood	Interstitial Fluid
Composition	Acellular, low protein content (0.2 g/L) (Di Terlizzi and Platt, 2006)	Plasma, red blood cells, white blood cells, platelets	Water, ions, gaseous molecules, organic molecules (Lei et al., 2017)
Originates	Choroid plexus and ependymal lining cells of the brain's ventricular system (Bedussi et al., 2018; Di Terlizzi and Platt, 2006)	(Supplied by) Internal carotid and vertebral arteries	From CSF, cell metabolism, vascular system (Lei et al., 2017)
Drains	Meningeal Lymphatics (Absinta et al., 2017; Aspelund et al., 2015)	Internal jugular veins (Doepp et al., 2004)	Into Ventricles and subarachnoid CSF (Begley, 2004)
Average fluid velocity	~5–8 cm/sec (human) (Battal et al., 2011)	0.9–5.5 $\mu\text{m/s}$ (mouse) (Bedussi et al., 2018)	10.5 $\mu\text{m/min}$ (cats) (Bulk flow)
Cerebral (Perivascular/capillary/interstitial) flow velocity	18.7 $\mu\text{m/s}$ (mouse) (Mestre et al., 2018a)	0.79 mm/sec (rat) (Ivanov et al., 1981)	.61–.86 mm/hr (rats) (Geer and Grossman, 1997)
Characterization of flow around tumor boarder	n/a	2.21–6.31 mL/100 mL (human) (Wu et al., 2016)	0–2 $\mu\text{m/s}$ (mouse) (Kingsmore et al., 2018)
Average volumetric flow rate	3.97 \pm 1.62 mL/min (depends on location) (Zhu et al., 2006)	236 \pm 9 mL/min (Sato and Sadamoto, 2010)	0.1–0.3 $\mu\text{L min}^{-1}$ g $^{-1}$ in rat brain; (Abbott, 2004)
Driver of flow	Arterial pulsatility (perivascular) (Mestre et al., 2018a)	Cardiac pulsatility	Arterial pulsatility (Rennels et al., 1990)
Diseases that affect flow and corresponding volumetric flow rate	Alzheimer's disease, Hydrocephalus (Linninger et al., 2007; Simon and Iliff, 2016)	Alzheimer's disease, Dementia, Parkinson's disease Schizophrenia Bipolar disorder, depression, Gliomas, Ischemic strokes, (See Review Fantini et al., 2016)	Strokes, Glioblastoma, Amyloidoses (Alzheimer's Disease, Cerebral Amyloid Angiopathy) (Arbel-Ornath et al., 2013a; Kingsmore et al., 2018)
Physical Properties			
Density	1006–1007 kg/m ³ (Levin et al., 1981)	1060 kg/m ³ (Cutnell and Johnson, 1998)	1000 kg/m ³ (Yao et al., 2012)
Viscosity at 37 °C	0.7–1.0 cP (Bloomfield et al., 1998)	1.3 \pm 0.1 cP (Tomiya et al., 2000)	3.5 cP (Yao et al., 2012)
PO ₂	65–130 mmHg depending on location (Zaharchuk et al., 2005)	173 \pm 25 mmHg (Tomiya et al., 2000)	Healthy: 22–40 mmHg Tumor: 0.5–27 mmHg (Helmlinger et al., 1997)
pCO ₂	55 mmHg (Andrews et al., 1994)	40 \pm 3 mmHg	77–95 mmHg (Voipio and Ballanyi, 1997)
pH	7.31 (Andrews et al., 1994)	7.45 \pm .04 (Tomiya et al., 2000)	Healthy: 7.1–7.5 Tumor: 6.6–7.4 (Helmlinger et al., 1997)

highlight the available techniques to measure fluid flow in the brain and discuss the impact that various techniques can provide.

2.1. Imaging modalities

2.1.1. Magnetic resonance imaging (MRI)

Magnetic resonance imaging (MRI) is a technique that has been used to measure cerebrospinal, blood, and interstitial fluid flow. Its non-invasiveness, tunability (i.e. fMRI, diffusion weighted, T1 and T2 weighted, Phase contrast), lack of radiation, and its compatibility with soft tissues makes it favored in the imaging of the brain (See Table 2 for a comparison of imaging modalities). MRI uses a strong magnetic field (~0.5–1.5 T) to align the axis (phase of rotation) with the protons in water molecules (Lotz et al., 2002). These protons are largely contained within the water molecules, which makes it ideal to measure tissues with high water content, like the brain. A paramagnetic contrast agent,

such as Gadolinium - Diethylene Triamine Pentaacetic Acid (Gd - DTPA), is often used to highlight areas of interest or see more defined structures (Berger, 2002). MRI is used clinically to diagnose diseases such as hydrocephalus, epilepsy, infections, strokes, brain tumors, disorders of the eye and many more.

This technique is advantageous because a radioactive injection is not required for tissue contrast, however, MRI is significantly more expensive and a much slower imaging modality than both x-ray and computed tomography (CT), requiring 2–3 h to scan the entire body. For these reasons, MRI is not an ideal imaging modality for quick feedback that may be desired during surgical procedures. Further, MRI should not be used if metal is used or implanted, as the strong magnetic field will dislodge any metal from the animal or patient.

2.1.2. Intravital microscopy

Optical intravital microscopy (IVM), similarly to MRI, can be used

Table 2
Overview of imaging modalities that have been used to measure fluid flow in the brain.

Modality	Fluids that can be measured	Ideal Tissue	Mechanism	Advantages	Disadvantages
MRI	CSF, ISF, CBF	Soft tissues, ligaments	Strong magnetic fields alter the spin of protons	No patient exposure to radiation	Slow, expensive
Intravital microscopy	CSF, CBF	Vasculature close to surface	Multiphoton, confocal microscopy often coupled with a cranial window (for the brain)	In vivo imaging, can track blood flow velocities in capillary sized vessels	Depth restrained to approximately 1 mm below surface, no clinical application
Nuclear Medicine (PET)	CBF	High metabolic regions, relatively non-specific	Radioactive tracer releases positrons read by detector	Detects changes in activity and function of tissue. In comparison to SPECT: fewer artifacts, high resolution, quantifiable	Patient is exposed to radiation. In comparison to SPECT: more expensive, fast half-life of tracer leads to short window for imaging
Nuclear Medicine (SPECT)	CBF	High metabolic regions, relatively non-specific	Radioactive tracer releases gamma rays read by detector	Detects changes in activity and function of tissue. In comparison to SPECT: Long imaging times, cheaper and more abundant radiotracers	Patient is exposed to radiation. In comparison to PET: cheaper, lower resolution, prone to artifacts,
Transcranial Doppler	CBF	Well characterized vessel location	Sound waves reflect off blood cells revealing speed and direction	Non-invasive, real time	Limited to measuring only blood flow velocities in arteries

to quantify CSF, CBF, and ISF flow velocities (Gabriel et al., 2018). For this technique, two photon confocal microscopy is coupled with a cranial window to track fluorescently labeled cells or beads to view the parenchyma and vascularity of the brain (Arbel-Ornath et al., 2013).

Due to the tissue being *in vivo* and uncleared, the restraining depth of imaging is about 1 mm, which still exceeds standard confocal microscopy. Though this technique can measure velocities at the capillary scale, it has little direct clinical application, as direct visualization of the brain is required.

2.1.3. Nuclear medicine

Regions of high blood flow can be correlated to regions of high activity, which is the basis for both fMRI, PET, and SPECT. Functional-MRI (fMRI) is a common way for scientists to study metabolism and brain activity, which is proportional to higher levels of blood flow. fMRI is frequently used to measure functional connectivity, which, reflects the spatial and temporal interactions between different areas of the brain (Smitha et al., 2017; Stephan and Friston, 2010). Positron emission tomography (PET) is similar to fMRI in that it produces qualitative images of high blood flow volumes that can, in turn, be manipulated to produce quantitative measurements. In contrast to fMRI, PET requires the injection of a radioactive tracers that produce positrons during decay, which exposes the patient to radiation (Lameka et al., 2016). Regions of high positron emission can be correlated to regions of high metabolism. This allows for a straightforward approach for tumor detection because they are more metabolically demanding than their physiologic surroundings. Similarly, blood flow volumes can be measured by the radioactivity of blood and local tissue (Herscovitch et al., 1983). Single-proton emission computed tomography (SPECT) is another form of nuclear medicine that requires the use of a radioactive tracer, except radiotracers for SPECT are far more common and have much longer half-times to increase imaging time. A full overview of the advantages and disadvantages of PET and SPECT can be found in Table 2, however one key takeaway is that PET is advantageous in that it can provide a quantitative measure of brain metabolism (Devous, 2005). Both PET and SPECT can be used in tandem with a Computed Tomography (CT) scanner to provide more detailed anatomical information. Inhalation of Xenon 133 is often used as an independent radiotracer to measure cerebral blood flow as it is easy collimated for *in vivo* quantification (Veall and Mallett, 1965), however this technique is primarily used to image the lungs. There are other techniques, such as Quantitative Autoradiography, that can visualize fluid flow pathways *ex vivo* by producing an image from the decay of the radioactive material injected within the tissue.

2.1.4. Transcranial Doppler (TCD)

TCD uses sound waves to evaluate blood flow velocities through, in, and around the brain. In brief, a pulsed wave is emitted, received, and reflected off red blood cells, which provides both a quantitative and qualitative output. Although this method is safe, non-invasive, and relatively cheap, there is a high degree of inaccuracy (5–20 %) because the readings are dependent on identification of the precise location of the intracranial arteries of interest (Sarkar et al., 2007).

2.2. Application of techniques to flows in the brain

Fluid flow in the brain is complex and consists of multiple compartments. Techniques that are applicable to one compartment, flow velocity, or geometry may not be the best tool for another. The ability to image and replicate measurements of flow within and around the brain is integral in clinical diagnosis and in development of new hypotheses in disease. Imaging each fluid compartment presents with its own set of challenges and outcomes, and thus they will be discussed separately.

2.2.1. Cerebrospinal fluid flow

Cerebrospinal fluid (CSF) is a clear colorless liquid that is constrained to the brain and spinal cord. CSF circulates within the hollow spaces of ventricular system. Although CSF is in close proximity to other fluids (*i.e.* CSF-ISF exchange and CSF-CBF barrier) it does not contain bulky proteins or red blood cells, thus measurement techniques such as Doppler cannot be used. CSF is created and removed only within the nervous system, and has fluid velocities and total volumes markedly higher than other fluids in the brain. The pulsation phase is crucial to accurately calculate the velocity of fluid flow because the phase shift is proportional to velocity. For this reason, Phase-Contrast MRI (PC-MRI) is among the most popular techniques to measure fluid flow in the brain and is most frequently used to measure CSF velocities. A recent study conducted by Boye et al. (Boye et al., 2018) combined PC-MRI with diffusion weighted MRI to develop the first, non-invasive method for the quantification of CSF flow in the subarachnoid space of the optic nerve finding glaucoma patients have decreased CSF flow compared to healthy patients.

Another common MRI technique is CINE PC-MRI, which is a combination of two tools, phase contrast and cardiac cine MR, first described by Nayler et al. (Nayler et al., 1986) that can depict motion and flow through the cardiac cycle (Pelc et al., 1991). CINE PC-MRI is frequently used because it provides an intuitive way to visualize and measure fluid motion by accumulating static PC-MRI images into a video. The output from this technique is a set of data that can depict obstructions, alterations, or excessive turbulent flows by quantitatively providing flow velocity measurements in all three dimensions (Quencer et al., 1990; Linninger et al., 2007). The spatial resolution of cine-MR in current studies allow for patient-derived geometries, as can be seen in the work by Linninger et al., where they utilized this technique to accurately measure patients' individual brain geometries and the CSF flow velocities in select regions of interest (Linninger et al., 2007).

CSF flow is reliant on multiple factors, such as cardiac pulsations, inhalation, and brain position. Cardiac pulsations have been historically accepted as the driver of CSF flow (Pelc et al., 1991) but recently, researchers have found that inspiration may also be a major regulator. As cardiac pulsations have some effect on CSF movement, a common technique to measure CSF flow is to synchronize the electrocardiogram to phase contrast MRI sequences (cardiac-gated PC-MRI), which confines the observation of CSF flow to the periodic heart rate (Wählin et al., 2012). However, Dreha et al. (Dreha-Kulaczewski et al., 2015) discontinued this trend by utilizing high-resolution, real-time magnetic resonance imaging (RT-MRI) to find that CSF flow may be influenced by inhalation. From these studies, it is now best to track both the cardiac gating and respiratory cycles throughout the MRI scan. In a recent study by Lindström et al. (Lindström et al., 2018), researchers used cardiac gated PC-MRI to conclude that when patients lie in the supine position, the spinal canal may be the net producer of CSF, as opposed to the choroid plexus. This response may serve as a means to keep ISF pressure homeostasis, as CSF pressure has been shown to be dependent on the position of the head with respect to the rest of the body (Klarica et al., 2006).

Being able to measure healthy flow velocities, total fluid volumes, and physical properties in CSF allows for the identification of abnormalities. For instance, physical properties of the fluid can help detect diseases. Protein concentrations are important considerations when measuring CSF, as variations can be indicative of diseased states (Paterson et al., 2019), and can also alter the movement of the fluid by increasing density or viscosity. In a healthy state, CSF should contain a small amount of protein, as serum proteins are often too large to cross the blood-brain-barrier, however protein levels in CSF increase in tuberculosis meningitis (Chin, 2014). Other characteristics such as fluid volumes are strictly regulated; understanding the intricacy of volume changes can be useful in diagnosing diseases that are correlated with CSF transport (Wählin et al., 2012).

Although the exact pathway of exchange between CSF and ISF is

unknown, there is strong evidence that these fluids mix in the perivascular spaces and that flow in these regions plays an important role in the removal of waste from the brain (Iliff et al., 2012). Mestre et al. measured CSF flow velocity through particle tracking velocimetry in the perivascular space *in vivo* and validated particle locations through *ex vivo* tissue staining (Mestre et al., 2018a). Increases in blood pressure lead to changes in vessel dynamics and in turn reduces perivascular pumping, decreasing the net flow of CSF in perivascular spaces, which are crucial brain clearance pathways of Amyloid beta. Thus, increasing flow of CSF through the brain by manipulation of drainage pathways can ameliorate the cognitive symptoms of AD (Da Mesquita et al., 2018a, Da Mesquita et al., 2018b). These flows were measured using dynamic contrast enhanced MRI (DCE-MRI) to track the movement of contrast agent through the brain parenchyma.

Some diseases are marked by an increase in CSF flow. Hydrocephalus, for example, is defined by an excess buildup of CSF in the ventricles of the brain and is diagnosed using MRI imaging (Nassar and Lippa, 2016). There have been a number of studies focused on comparing fluid flow velocities in various regions of the ventricular system of a healthy and hydrocephalic patient. A study by Linninger et al. utilized CINE-MRI to determine that CSF flow patterns in hydrocephalic patients can increase by 2.7 times (Linninger et al., 2007). Lindström et al. used PC-MRI to measure CSF flow in both asleep and awake idiopathic Normal Pressure Hydrocephalus (iNPH) patients. They found that CSF volumetric flow was retrograde and significantly higher than in healthy counterparts at the cranio-cervical junction (Lindström et al., 2018). Thus, both high and low CSF flow rates are correlated with diseases in patients, yet inpatient heterogeneity remains high.

2.2.2. Cerebral blood flow

Cerebral blood flow (CBF) is closely coupled to glucose and oxygen metabolism (Liang et al., 2013), which is reflected by the most common measurement techniques that are used. CBF is unique in that blood circulates systemically, thus a specific barrier, the blood brain barrier, is required to regulate what is permitted to enter the interstitial spaces. Discontinuation, disruption, or obstruction of CBF has severe consequences in cognitive function, thus, autoregulation within the brain results in a constant blood supply regardless of changes in perfusion pressures (Fantini et al., 2016; Miller et al., 1993). Studies have shown that this autoregulation exists at the capillary level where astrocytes respond to vasoactive molecules and signal contractile smooth muscle cells to regulate blood pressure (Kimbrough et al., 2015). Because the velocities for CBF have a range of size scales from cerebral arteries to capillaries, a range of methods are often used to measure regional and local CBF.

Functional imaging is often used to assess regional changes of total blood flow in the brain. Liang et al. (Liang et al., 2013) utilized fMRI to show that blood supply is dependent on roles of the brain regions, meaning that higher tasked regions are supplied by higher levels of CBF. A variety of radioisotopes with PET imaging have been utilized to examine total blood flow. For example, Frackowiak et al. combined the inhalation of the positron emitting radioisotope of oxygen, ^{15}O , with PET to develop a method to measure regional CBF and oxygen consumption (Frackowiak et al., 1980). Combining PET with SPECT to study CBF in patients was approximately 88 % accurate in diagnosing AD (Bonte et al., 2006; Brooks, 2005).

TCD can more directly measure blood flow velocities and shows promise in predicting acute strokes when measured in the middle cerebral artery (Alexandrov et al., 1994). A compromise between SPECT and TCD, would be cerebral angiography, which uses x-rays and an iodine-containing contrast agent to view the blood vessels in the brain, with comparable, but improved, outcomes seen in TCD (Lysakowski et al., 2001). For CBF traveling through capillaries or arterioles, intravital imaging can be used, as this technique allows for individual cell tracking, of red blood cells, for instance, to calculate velocities through

a vessel in mice (Kimbrough et al., 2015).

Changes in CBF have been recently implicated in a number of diseases associated with cognitive decline as highlighted in the review by Ogoh et al. (Ogoh, 2017). Often flow is obstructed by vascular amyloid, which are luminal amyloid beta accumulations that cause vasoconstriction as the deposits narrow the lumen of cerebral vessels (Crawford et al., 1997). Using a novel, *in vivo*, multi-photon imaging technique through a cranial window, scientists found that vascular amyloid interfered with the signaling pathway in the gliovascular unit. This disruption in signaling may contribute to cerebral hypoperfusion in AD and associated cognitive deficits (Kimbrough et al., 2015). More recent studies using PC-MRI support this finding of cerebral hypoperfusion indicating both blood flow total volume and velocity were decreased, emphasizing that a decrease in blood flow correlates with the degree of cognitive impairment (de Eulate et al., 2017).

As mentioned, these fluid flows are not independent in the brain. A study by Owler et al. utilized ^{15}O -water PET with MRI to study the reaction of CBF after variations of CSF, to mimic the environment found in NPH. They found that increased CSF pressure correlated to a decreased global CBF, with the most significant decrease in blood flow occurring near the ventricles. This is thought to be either from a direct compression of the cerebral tissues, inhibiting blood flow, or, more probable, increased interstitial fluid was compromising CBF (Owler et al., 2004). Thus, though CSF and CBF are often measured or studied independently, they are closely linked.

2.2.3. Interstitial fluid flow

The interstitial space within the cerebral tissue also has fluid flow within it, though this flow is much slower than that of CSF or CBF, leading to many molecules moving more by diffusion than with fluid flow. Interstitial fluid (ISF) surrounds every cell in the brain, allowing it to be the main carrier for proteins trafficking to and from cells. ISF flows in the paravascular space, known as Virchow-Robin spaces, which exist around blood vessels of the brain that are bounded by one or more leptomeningeal layers. ISF flow around these vessels reaches terminal capillary beds, which serves as an exchange site for ISF and CSF (Iliff et al., 2013). This space plays a crucial role in the removal of waste from the brain and due to this role, it has been termed the “glymphatic system”. Movement of fluid within this system has been imaged using MRI with contrast agent and through use of fluorescent tracers and intravital imaging (Feng et al., 2013; Harrison et al., 2018). Through these imaging techniques, the glymphatic fluid flow is thought to be driven by influx of fluid from the gliovascular unit (Iliff et al., 2012). More recently, the glymphatic system has been determined to drain to the lymphatics that were identified as surrounding the brain in the meningeal layer. Once again, MRI with contrast was used to see this fluid movement and subsequent drainage into deep cervical lymph nodes (Eide et al., 2018).

ISF can be measured either flowing through the paravascular spaces or through interstitial spaces between cells in the parenchyma. This latter flow has mostly been implicated in brain tumor biology. Geer & Grossman utilized Quantitative Autoradiography to determine ISF flow pathways that could be generated by increasing interstitial pressures similar to those caused by tumor growth. Based on transport of tritiated inulin in sequential slices both anterior and posterior to the injection site, they found that the average ISF flow rate ranged from 0.61 to 0.86 mm/h (Geer and Grossman, 1997). This technique requires tissue slices, thus cannot be performed *in vivo*, however, has high sensitivity and resolution. More recently Aspelund et al. measured ISF through the interstitial space by tracking the flow of PEG-IR Dye immediately after injection in ex vivo tissue slices (Aspelund et al., 2015).

MRI has proved useful in measuring ISF flows. Tracer based MRI can delineate ISF flow and drainage pathways via injection of Gd-DTPA, and sequential T1-weighted MRI (DCE-MRI) to track its movement (Han et al., 2012). Using a similar technique with implanted glioma in mice, it was seen that adjacent flows are disrupted near tumors (Guan et al.,

2017). Kingsmore et al. expanded on this technique to use mass transport to calculate ISF rates in and around brain tumors, which further supported the disrupted flows and highlighted the complexity inherent to ISF in and around developing brain tumors (Kingsmore et al., 2018). Kingsmore et al. utilized Spin Echo MRI to measure ISF flow influx and outflux of a brain tumor as it is able to detect diffusion (Tanner and Stejskal, 1968). This is an important element in the measurement of ISF flows as often they are of a similar magnitude to movement of the contrast agent by molecular diffusion, or random motion, alone.

Diffusion tensor imaging (DTI), or more broadly diffusion-weighted MRI (DW-MRI), is a method to measure flow in the brain that is sensitive to net water displacement (Basser et al., 1994). Most common for measuring and mapping white matter tracts within the brain, Harrison et al. used this method to detect ISF flow in the paravascular space, which, before this point could only be measured through injection of contrast agents (Harrison et al., 2018). Using the same technique, impaired glymphatic clearance was observed not only in diseases such as AD but also in hepatic cirrhosis (Hadjihambi et al., 2019).

Measuring the magnitude and velocity of ISF flow in both the healthy and diseased brain is important for drug applications, disease treatment, and prevention (Han et al., 2012). It is well known that there exists a vital exchange between CSF and ISF in the network that plays a substantial role in the removal of Amyloid beta (Iliff et al., 2012; Bedussi et al., 2015). Arbel et al. used real time *in vivo* measurements via a cranial window to find that stroke increases the long term risk for AD (Arbel-Ornath et al., 2013). Using a fluorescent molecular tracer with a similar mass to Amyloid beta with multiphoton time lapse imaging they found reduced efficiency of clearance of the tracer through the ISF pathway when they induced ischemic strokes. This demonstrates that for ISF to effectively drain Amyloid beta proteins, vasculature needs to be functional. Thus, not only is ISF-CSF exchange important, but ISF-CBF connections are also integral to normal function in the brain.

ISF flow plays a role in glioma cell invasion (Kingsmore et al., 2016; Munson et al., 2013). Thus, in glioma, the group utilized Spin echo MRI to detect Gadolinium intensity differences over time. They accompanied their MRI measurements with an *in vitro* tumor microenvironment phantom to validate the flow velocities obtained through the scan. Through this novel and noninvasive method, ISF flow velocities can be measured directly *in vivo* in GBM. Kingsmore et al. found that the direction of fluid flow is heterogeneous within and around the tumors and is not always in the outward direction (Kingsmore et al., 2018). These heterogeneous flow pathways were further investigated to determine that Glioma cells are flow responsive and may act as a predictive marker for Glioblastoma invasion via CXCR4 dependent mechanism (Munson et al., 2013). It is well known that the interstitial pressure is higher in the tumor than in the surrounding healthy tissue (Boucher et al., 1990). However, when Munson et al. (Kingsmore et al., 2018) measured ISF velocities, they found that there was not a significant correlation between the tumor size and the ISF velocity, which does not support the previous findings that larger tumors have corresponding higher ISF pressures (Boucher et al., 1997). Current theories suggest that, instead, there may be an upper threshold for interstitial flow velocities in these confined spaces of the brain, which requires further investigation during the development of this disease.

3. Modeling fluid flow in the brain

The measurement of fluid flow in brain is instrumental in helping us understand and diagnose conditions with obstructed or abnormal flows. These measurements are also useful for creating models of healthy and diseased brain such that we can discover new mechanisms or identify new therapeutics to address neurological disorders. These realistic measurements when coupled with mathematical or computational models which solve the fundamental governing equations of fluid

dynamics can predict the velocity, pressure and other variable physical properties. These models in turn, offer a useful tool in not only understanding the flow but also to analyze, non-invasively, how the changes in these physical properties affect the normal brain functions and fluid transport. An ideal example would be the study conducted by (Rey and Sarntinoranont, 2018) who modeled arterioles with and without veins along with the surrounding perivascular spaces and brain parenchyma to study the effects of varying certain parameters of the model on fluid transport. Measurements can also be helpful in the creation of *in vitro* platforms that incorporate fluid flow. These can be integral for the screening of new compounds or testing specific hypotheses in a defined environment (Tate and Munson, 2019). The following section addresses the recent attempts at modeling the fluid flow in the brain.

3.1. Computational/ mathematical models

Mathematical or computational fluid dynamics (CFD) models when conducted with physiologically realistic parameters and boundary conditions (the values of the physical properties at the boundaries of the domain of fluid flow) along with patient derived data, can reveal vital information about the different types of fluid flows in brain which is difficult to obtain *in vivo*, due to the anatomical barriers that prevent or at least make it difficult to reach the internal regions. Thus, these models have been extensively used to understand the underlying mechanisms that govern flow, to study their behavior under normal and pathological conditions and to investigate how the changes in their behavior can lead to certain abnormalities and vice-versa. (Grinberg et al., 2009a, 2009b) and (Perdikaris et al., 2016) have performed some extensive modeling of the cerebral blood flow in the intracranial arteries combining different length scales, the details of which will be addressed later in the review. These models are useful tools to not only study the fluid or flow properties, but can enable the user to modify the values of different physical parameters (*i.e.* fluid density, tissue permeability) and constants to observe the effects of resulting changes. In this way, we can learn more about the physiology of disease and identify emergent phenomena independent of laboratory experimentation.

3.1.1. Cerebrospinal fluid flow

As mentioned, a disruption in CSF flow plays a part in AD and hydrocephalus. Thus, detailed computational and mathematical models of the flow including its point of origin at the choroid plexus and its flow path through the brain ventricles and the subarachnoid space, is capable of predicting the changes in its properties caused by pathological conditions. The models when coupled with physiologically realistic or patient derived data (on boundary conditions and geometry) the *in vivo* values of which can be obtained from different measurement techniques (discussed in the earlier section) can help in understanding the normal and abnormal flow dynamics in stable or diseased conditions.

Gupta et al. developed a comprehensive three dimensional CFD model of CSF flow in the subarachnoid space using a model geometry created from patient specific data obtained from MRI images (Gupta et al., 2010). They created a model which coupled a model of porous medium using the Brinkman equations with the fundamental Navier-Stokes momentum equations for one complete cardiac cycle. This resulted in velocity and pressure contour maps to show that the CSF pressure gradient is affected by changes in trabecular morphology. The same group also modeled the pulsatile CSF flow in the inferior cranial space and superior spinal subarachnoid space again using patient-derived boundary conditions revealing that the pressure varied from -42 Pa to 40 Pa (Gupta et al., 2009). Varying CSF velocities from 15 cm/s in the inferior aqueduct to 9 cm/s in the foramen of Magendie indicated the presence of a three-dimensional brain asymmetry. By using patient-specific geometries of the CSF-filled spaces, modelers were able to match velocities as determined from Cine PC-MRI (Sweetman et al.,

2011). The changes in the properties of CSF flow, such as absorption resistance, play a role in pathological conditions. A computational model of intracranial dynamics predicted these changes in CSF flow that mark the onset of the disease (Linninger et al., 2009). This dynamic model including the CSF, brain parenchyma, the vascular system and the spinal canal, utilizes fundamental mass and momentum conservation equations to predict the rates, velocities and pressure gradients of blood and CSF flow. The pulsatile CSF flow in brain ventricles, the subarachnoid space and parenchyma modeled using patient-specific brain geometries correctly predicts the flow and pressure fields under normal and hydrocephalic conditions (Linninger et al., 2007). Similarly, information on the decrease in the size of the lateral ventricles can be used along with velocity data obtained from time-resolved phase contrast images to build a mathematical model capable of predicting the CSF flow dynamics in normal and hydrocephalic patients (Zhu et al., 2006).

A CFD model of CSF flow through the four brain ventricles along with their connecting pathways is a useful tool to investigate the effects of a stenosed aqueduct on the pressure propagation between the third and lateral ventricles (Kurtcuoglu et al., 2005). This model where the fluid flow is driven by a predefined sinusoidal motion of the lateral walls of the third ventricle showed the effect of the condition of the aqueduct of Sylvius (*e.g.* if there is stenosis) on the pressure amplitude in the lateral ventricles. Lastly, a subject specific CFD model of CSF flow in the third ventricle and aqueduct of Sylvius was constructed by incorporating boundary conditions and realistic domain geometry data from MRI scans (Kurtcuoglu et al., 2007). The results showed the emergence of a fluid jet from the aqueduct of Sylvius with mobile recirculation zones above and below it. The properties of CSF and other fluid compartments of the brain are closely related as was shown by the mathematical model developed by (Ursino and Lodi, 2017). Through development of a complex multicompartiment model, they explored the relationship between CSF, the intracranial pressure and the dynamics of arterial blood flow under different conditions. These complex models have promise for offering a more complete picture of intracerebral fluid movement, but are exceedingly difficult to develop, implement, and validate.

3.1.2. Cerebral blood flow

Modeling the CBF requires the incorporation of multiscale vascular networks due to the branching and extensive nature of the brain capillary network. A comprehensive and physiologically realistic model of the vascular network of brain is required to capture the difference in fluid dynamics at different scales starting from the macro scale comprising the larger arteries of up to 0.5 mm diameter, mesoscale arteries or arterioles ranging from 10 to 500 μ m in diameter up to the micro scale arterial network below 10 μ m diameter that consists of the capillary bed, while retaining the complexity in geometry. The most modeled component of the cerebral vascular system is the Circle of Willis (CoW), which is a ring like arrangement of vessels below the hypothalamus. The abnormalities in the structure and function of the CoW have been linked to different types of diseases like hydrocephalus and cerebral aneurysms. A detailed model of blood flow through the CoW can help us understand the complicated dynamics and the effects of abnormalities on the flow and *vice versa*. A two dimensional computational model of blood flow in the Circle of Willis allows the simulation of peripheral resistance together with auto-regulation and can be used to simulate the common abnormalities and their effects (Ferrandez et al., 2002). But, CFD modeling of entire human intracranial arterial pathway requires extensive computational capabilities that can cover the full range of dimensions starting from the macrovascular network to the fine capillary bed. To address this problem, while trying to model the flow in complete and incomplete Circle of Willis in healthy and hydrocephalic brains respectively, the authors, (Grinberg et al., 2009a, 2009b) used two level domain decomposition technique and a novel resistance-capacitance type outflow boundary

condition. The macroscale arterial network comprising of the larger arteries (0.5 mm in diameter) was simulated while the mesoscale (10–500 μm in diameter) and microscale networks (capillary bed) served as the boundary conditions. Apart from that, patient derived data was also used to model the geometry of the arterial network along with inlet boundary condition information which was obtained from *in vivo* flow rates. The simulation results show the presence of secondary flows in the communicating and internal carotid arteries for both healthy and diseased brains along with a high pressure drop along the pathway connecting the basilar and internal carotid artery in incomplete Circle of Willis model. A more advanced attempt at the reconciliation of the continuum and atomistic domains in one computational model was made by (Grinberg et al., 2012) where the authors studied platelet deposition and clot formation on the wall of brain aneurysm by using a coupled multiscale method where the higher order Navier Stokes solver NekTar was used for the continuum domain (regime at higher length scales where we can assume continuity of properties and neglect the variations due to molecular motions) and parallel code LAMMPS was used to account for the stochastic molecular dynamics regime (regime at very small length scale where it is necessary to consider the effects of molecular motions). The interface between the two domains was solved by adaptively computed effective forces that maintain continuity across the interface boundary condition. Thus, in order to model and understand the fluid dynamics in the entire intracranial arterial tree and study the effects of changes in the flow and structural properties under abnormal conditions, it is necessary to use advanced computing machinery that can simulate different length scales simultaneously with reasonable accuracy.

Multiscale models use patient derived geometry to compute the velocity or the flow fields of blood at different scales starting from an order of magnitude 0.1 mm in the continuum regime to 1 μm at the atomistic regime which captures the clot formation. In this context it is relevant to mention that an exhaustive review of the different attempts to computationally or mathematically model the blood flow in brain has been presented in (Perdikaris et al., 2016). The authors have covered the studies carried out till 2009 to analyze the blood flow dynamics in normal and diseased brains spanning the three different length scales of the intracranial arteries. Blood flow through three dimensional model of the intracranial venous network has also been modeled, by (Miraucourt et al., 2016) where they addressed all the aspects of modeling from development of geometry (from imaging data) to meshing and the governing equations. (Gadda et al., 2015) developed a lumped parameter model of outflow of cerebral venous blood. They simulated the pressures and volumetric flow rates through cerebral, vertebral and jugular ducts and analyzed the effects of posture changes and stenosis on these variables. So, equipped with realistic and patient derived geometry, CFD is thus, an efficient tool to analyze dynamics of cerebral blood flow in brains performing normal functions as well as the ones with vascular diseases like giant in transcranial aneurysm (Steinman et al., 2003). But in order to obtain accurate results from computational modeling of blood flow we need not only patient derived realistic values of parameters but also efficient computational capabilities that can model entire flow paths with equal precision simultaneously to promptly see the global effects of local changes.

3.1.3. Interstitial fluid flow

Modeling of the ISF in the brain parenchyma can be useful for developing an understanding of not only how drugs and nutrients are transported in and around cells, but also the types of mechanical forces that cells feel. Multiple Network Poroelastic Theory (MPET) is a useful tool to study the material exchanges between the CSF, blood and the brain parenchyma containing the interstitial fluid and this mathematical model can be used to test and analyze the changes in the cerebral physiology and fluid flow properties that contribute to NPH (Tully and Ventikos, 2011). A lot of studies aimed at investigating the ISF flow, have taken into account the effects of direct brain infusion, the results

of which are relevant for drug delivery (Kim et al., 2012) & (Dai et al., 2016). The origin and transport of the ISF in brain have long been the subject of research (Abbott, 2004). Evidence supporting a model of the volume regulation of brain CSF was presented by (Cserr, 1988). The model incorporates the fluid exchange process between the blood, the brain parenchyma and the surrounding space filled with CSF. According to this model, the total volume of the brain interstitial fluid is maintained by its secretion at the blood brain barrier and its exchange in bulk with the surrounding CSF spaces. Another example is a mathematical model of infusion induced swelling in the brain tissue which revealed the important characteristics of the changed interstitial flow as a result of the infusion (Baser, 2019). Treating the condition as fluid flow through poroelastic medium, the pressure, velocity and volume distribution plots showed different volume concentrations in the tissue with the maximum occurring at the site of infusion. The model which also incorporates solute transport equation, can be used to calculate other physical properties of the brain tissue. An individual specific model of fluid infusion into brain that took into account the heterogeneity of different regions and their responses to the infusion showed good agreement with experiments that used the distribution of tracer molecules (Raghavan and Brady, 2011).

The human brain tissue is a heterogeneous mass comprising of tissue cells and blood vessel walls. This multicomponent domain, permeated by blood and interstitial fluid has been modeled along with tissue characteristics obtained from medical imaging (Ehlers and Wagner, 2015). Direct tissue infusion of therapeutic agents have been tested by the model by treating the interstitial fluid as a mixture of liquid solvent containing dissolved solute. Mathematical or computational modeling of interstitial flow in brain parenchyma in pathological conditions for example in tumors, also reveals the associated changes in the properties of the fluid or the flow. The interstitial fluid pressure is usually elevated inside the tumor mass due to abnormal growth and congestion of cells and leaky vasculature formed as a result of tumor associated angiogenesis. This elevated pressure causes a flow from the tumor towards the surrounding interstitial space thus aiding the process of invasion and metastasis of cancer cells (Fig. 2). Numerical modeling of a uniformly perfused tumor shows that radially outward increase in convection inside the tumor, along with non-uniform filtration of substances from the vessel walls and reduction in extravasation force results in a heterogeneous arrangement of macromolecules (Baxter and Jain, 1989).

The modeling of the three main types of fluid flows in brain along with physiologically realistic parameters and conditions in healthy and diseased brains can reveal and explain certain phenomenon that is difficult to address *in vivo*. But a thorough modeling can predict *in vivo* conditions only when it incorporates patient derived geometries, boundary and initial conditions, uses realistic parameter values and addresses the relevant solid and fluid physics at that particular scale. Lastly, the model generated results should be compared with those obtained *in vivo* or in clinical settings to check their precisions and accuracies. An area of potential opportunity for new models is a multiscale, multi compartment simulation that incorporates all three types of fluid flows along with the exchange of materials at the barriers. This type of comprehensive model might be computationally expensive but it will be able to answer, simultaneously, a number of different questions and help analyze the effects of changes in one fluid on the others as well as the entire brain.

3.1.4. In vitro microfluidic models

In vitro models of the brain that mimic the *in vivo* environment enable us to have a closer look at the effects of different cell, matrix and the fluid interactions. With the advancements in materials and micro-fabrication technologies, it is now possible to build microfluidic devices that precisely and accurately create, control and regulate the micro-environment that are involved in fluid flow in the brain. However, there are limited models that are specifically focused on recapitulating fluid

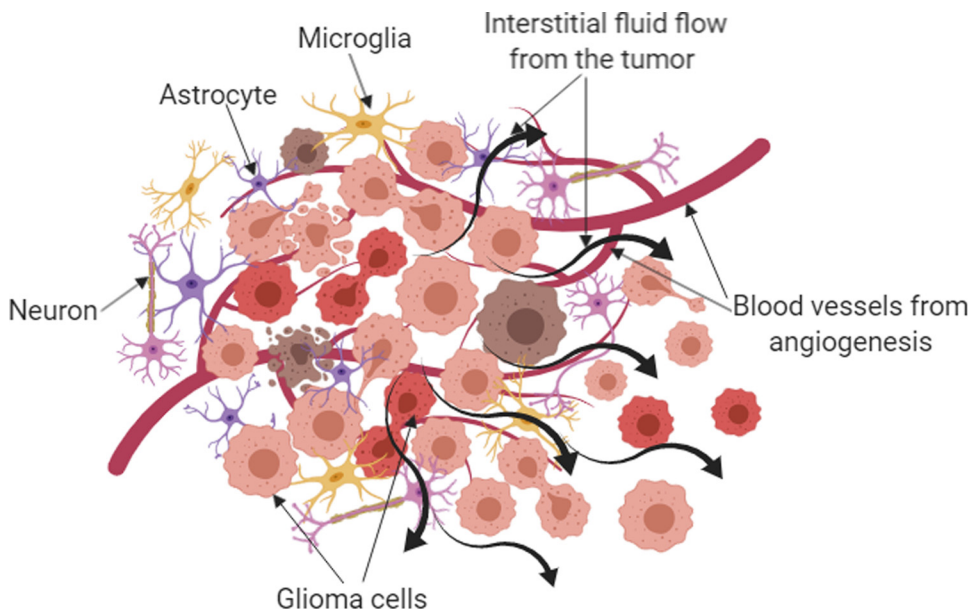


Fig. 2. Simplified depiction of glioblastoma microenvironment showing the different types of cells, vasculature and discrete fluid flow that may be present. Heightened pressure inside the tumor results in outward flow of interstitial fluid from the tumor edge towards the surrounding healthy tissue. This heightened flow has been shown to play a role in tumor cell invasion.

flow in this capacity.

3.1.5. Cerebrospinal fluid flow

The prevalence of studies exploring *in vitro* CSF models in existing literature is low. This may be due to long flow path of CSF, the large surface area that facilitates its exchange of substances with the interstitial space and the complicated geometries of many compartments (such as the subarachnoid space). Thus any model that tries to recreate the *in vivo* features in the CSF flow path has to incorporate physiologically realistic pressure at that particular location, proper arrangement of cells around the path, the exchange of substances with the brain parenchyma and the pulsatile nature of the flow. An attempt to recreate *in vitro*, some of the relevant *in vivo* physiological conditions, was made by culturing arachnoid granulation cells along with realistic intracranial pressure to build a model of the outflow pathway for the cerebrospinal fluid (Grzybowski et al., 2006). In order to do this, human arachnoid granulation cells were cultured on a membrane and perfused both in physiologic and nonphysiologic directions to study the effects of change in directions on transcellular pressure, flow rate and average hydraulic conductivity. The results demonstrated that the cells experience a greater flow rate and hydraulic conductivity under the more physiologically realistic conditions. In a somewhat related study, the important topic of contribution of CSF to the development of the cerebral cortex and its ability to maintain the viability of the cortical cells was investigated by combined *in vitro* studies and quantitative analysis of migration and proliferation of immunocytochemically stained cortical cells (Miyan et al., 2006). Thus, there is ample opportunity for development of novel models that incorporate and/or specifically model CSF flow.

3.1.6. Cerebral blood flow

In vitro models that try to mimic the cerebral blood flow primarily focus on the blood-brain barrier (BBB). The blood-brain barrier separates the blood in the microvessels and the ISF in the brain parenchyma. The tight junctions of the endothelial cells prevent the exchange of neurotransmitters and hydrophilic substances between the blood and the interstitial fluid in the brain parenchyma while astrocytic endfeet maintain and uptake molecules. Similarly, the blood-CSF barrier at the choroid plexus is made up of a tight layer of epithelial as well as capillary endothelial cells (Fig. 3). Thus, even though there is a lot of similarities in the composition of the CSF and the ISF, they differ significantly from the composition of blood plasma, which is due to the

presence of these barriers formed of tightly joined cells.

The BBB poses a challenge to drug delivery inside the brain as the only route of transport through the barrier is through the cells. *In vitro* microfluidic devices that capture the physiologically realistic *in vivo* conditions can be used as models to test the permeability of the barrier to drugs. One way of achieving this is to co-culture microvascular endothelial cells with primary astrocytes on both sides of a porous membrane and perfuse the device with nutrient rich medium at physiologically relevant rates in a pumpless microfluidic device as shown in Fig. 4A (Wang et al., 2017a). The barrier showed the formation of continuous tight junctions, which are essential features and *in vivo* like values of trans-endothelial electrical resistance (TEER). A model like this which can successfully mimic *in vivo* properties of the blood brain barrier could be used as an effective test bed for studying drug transport. A similar model was built by using a thin culture membrane to create a dynamic microenvironment by culturing bEND3 endothelial cells in the presence or absence of co-cultured C8-D1A astrocytes (Booth and Kim, 2012). Optical imaging, permeability assays and trans-endothelial electrical resistance were used in this study to test the physical properties of the barrier and extent to which the model could capture *in vivo* conditions. So, these types of microfluidic devices that use endothelial cells and astrocyte end feet that form the tight junctions are useful methods to manipulate the BBB properties especially for drug delivery testing.

3.1.7. Interstitial fluid flow

Creating an effective platform for investigating ISF flow effects require a 3D space through which fluid can flow around cells (glial cells and neurons) and through the extracellular matrix. These systems are useful for exploring the effects of ISF on the cellular morphology and behaviors as well as drug delivery through direct intracranial perfusion (i.e. convection-enhanced delivery). ISF was important to yield better neurospheroids and neural networks in a brain-on-a-chip microfluidic device which incorporated neurospheroids grown from neural progenitor cells as shown in Fig. 4B (Park et al., 2015a). These neural cultures were subsequently used to investigate the neurotoxic effects of synthetic amyloid- β and proved to be an efficient *in vitro* model of AD. The neurotoxicity of amyloid beta was also studied *in vitro* by using a microfluidic device capable of sustaining an interstitial level of flow (Choi et al., 2013). The results indicated that the increase in the number of fibrils did not have any effect on the neurotoxicity but the oligomeric assemblies of amyloid beta had an atrophy effect on the neurons

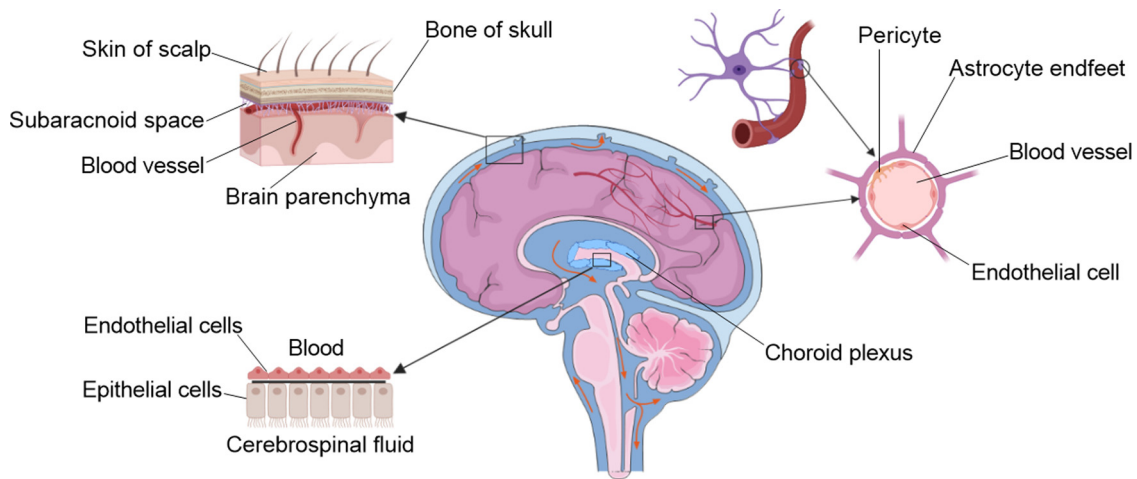


Fig. 3. Current understanding of the locations and cellular compositions of the barriers separating the three main fluids of the brain. The blood-brain barrier separates the blood in the vessels and the interstitial fluid in the brain parenchyma, the blood-cerebrospinal fluid barrier separates blood from CSF in the choroid plexus and the CSF-ISF barrier lies between the CSF in the sub-arachnoid spaces and ISF in brain parenchyma.

cultured in the microfluidic device with continuous flow. So, it is possible to achieve organ level details in a microfluidic device with cells and ISF, which can act as *in vitro* models of different neurodegenerative diseases appropriate for drug testing. Culturing brain tissue slices instead of cells is another option to create organ specific microenvironment and is popular in *in vitro* experiments in neuroscience but is limited to thin organotypic slices because of the difficulties in culturing thick slices. A thick tissue slice (700 μm) culture and maintenance requires a 3-D interstitial chamber capable of maintaining the perfusion of oxygenated nutrient rich medium along the entire surface and thickness of the tissue which could be achieved by a gas permeable microfluidic chamber equipped with forced convection based mass transport (Rambani et al., 2009).

Glioblastoma has been modeled with ISF most commonly due to the prevalence of heightened ISF around tumors in the brain. Glioma cells

embedded in a hyaluronan matrix respond to ISF by invading through a tissue culture insert system in a CXCR4-CXCL12 dependent manner (Munson et al., 2013). Using the same matrix in a microfluidic device, ISF caused tumor cells to both begin migrating and migrate directionally. Similarly, using a pump driven tissue culture insert system, Qazi and colleagues saw an increase in glioma cell invasion that was dependent on interactions with the glycocalyx (Qazi et al., 2013). Kingmore et al. found that both mechanisms can differentially regulate glioma invasion depending on the patient in a similar system (Kingmore et al., 2016). Thus, by incorporating ISF into a simple *in vitro* system, new targets against glioma invasion can be identified.

4. Manipulating fluid flow in the brain

Measurement and modeling of fluid flow is important for enabling a

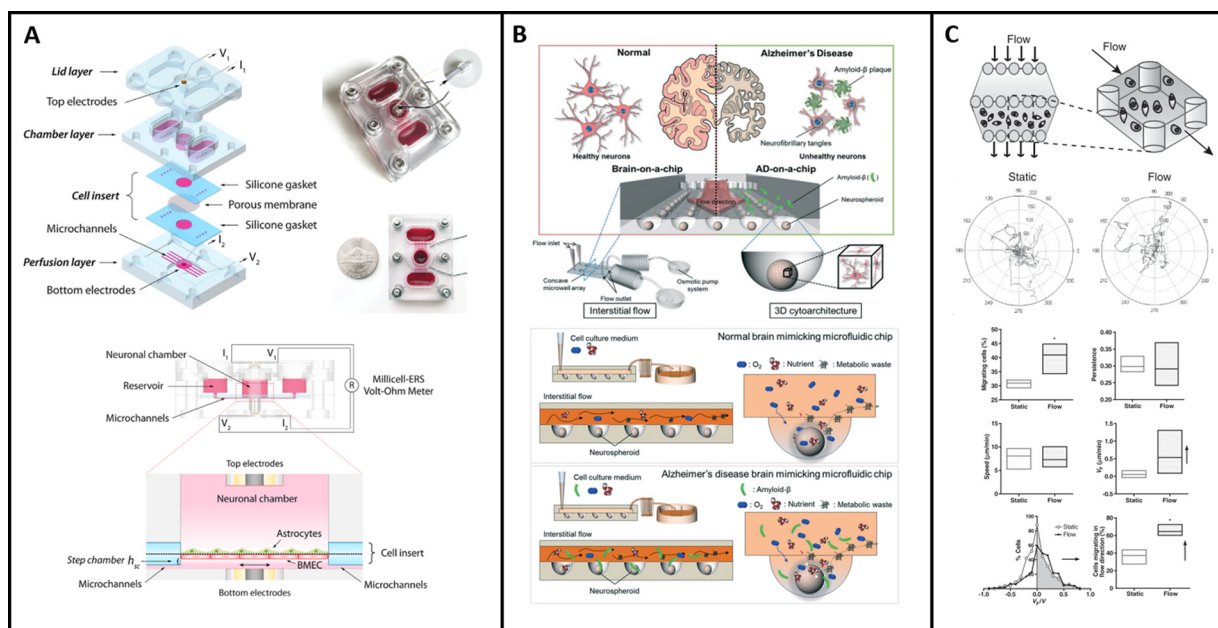


Fig. 4. Recent examples of *in vitro* models that incorporate elements of fluid flow within the brain **A.** Schematic and assembled view of Blood Brain Barrier on chip model by (Wang et al., 2017a). The side view and the zoomed in panel show the arrangement of cells, porous membrane and the electrical wiring. **B.** Schematic of the brain on a chip mimicking Alzheimer's disease by (Park et al., 2015a) and the comparison of neurospheroid formation between this device and a normal brain mimicking microfluidic chip. **C.** Schematic of the interstitial flow chamber and analysis of glioma cell migration under static and flow conditions (Munson et al., 2013).

better understanding of the interactions of anatomical structures with fluid dynamics. However, fluid flow in the brain is not a passive force, it is a force that interacts with cells and tissues in ways that contribute to morphological changes. During development neural stem cells follow flow within the brain to pattern within the tissue, glioma cells actively migrate in response to flow (Fig. 4C), and fluid flow actively transports amyloid beta plaques out of perivascular spaces (Sawamoto et al., 2006). Therefore, as we understand that flow is related to physiological changes and in mediating changes that correlate with disease, methods to alter flow can offer insight into causation of disease phenotype and potential therapies to correct aberrant flow.

4.1. Cerebrospinal fluid flow

Manipulation of the CSF has been mainly performed with the intention of measurement of different factors in normal or diseased conditions dependent on the flow properties (Lee et al., 2018). For example, a small molecular weight contrast agent Gd-DOTA was infused into the CSF of Wistar rats via the cisterna magna and gadolinium concentration maps of the whole brain were developed to estimate the solute uptake of the brain parenchyma. The maximal retention by the brain parenchyma was found to be 19 % of the amount delivered. The relationship of bulk flow of CSF into the brain with changes in plasma osmolality was measured by the perfusion of artificial CSF containing diethylenetriamine penta acetic acid (DTPA) and radio labeled albumin into the brain of anesthetized rats (Pullen et al., 2017). The clearances of albumin and DTPA from CSF to the brain were studied under the normal and hyperosmolar conditions and it was found that the tracer clearances increased in a rate similar to the osmolality though there was a seven fold difference in the diffusion coefficient. CSF flow compartments are lined with ependymal cells whose apical surfaces have cilia. The coordinated beatings of bundles of cilia are thought to play a role in the transport of CSF through the brain ventricles by forming a fluid flow network (Faubel et al., 2016). So, even though evidences suggest the role of changes in CSF properties and circulation in neurodegenerative and neuroinflammatory diseases (Simon and Iliff, 2016), it is difficult to manipulate the CSF flow without causing any collateral changes because of the vast expanse of its flow route, its location in numerous areas of the brain and the spinal cord and the continuous exchange of materials that takes place between the three different fluids.

4.2. Cerebral blood flow

Changes in properties and abnormal functionalities of cerebral blood flow have been known to be the root cause of a number of pathological conditions of the brain. Manipulations of the cerebral blood flow have been used extensively to study the effects of different external parameters on the flow and the subsequent effects on brain functions. The cerebral pressure autoregulation with corresponding changes in the cerebrospinal fluid pressure due to infusion were studied using O-water positron enhanced tomography and magnetic resonance imaging in patients with normal pressure hydrocephalus. Reduction in global as well as mean CBF in certain regions of the brain for example basal ganglia, thalamus, and white matter area had significant correlations with variations in the pressure of CSF (Owler et al., 2004). Post-operative changes in CBF were studied in patients who had undergone clipping of unruptured cerebral aneurysms by using two irrigation fluids, which are Artcereb and physiological saline. Territories near the parent artery, which underwent clipping showed more reduction in CBF especially during early postoperative period (Shimizu et al., 2011). Deep brain stimulation (DBS) targeting the ventral intermediate nucleus of thalamus is known to alleviate the symptoms of tremors. The mechanism of the operation of DBS and its effects on the function of neurons have been investigated by PET measurements of cerebral blood flow. The results show increased flow at the site of stimulation and in ipsilateral supplementary motor area containing afferent neurons from

the site of stimulation (Perlmutter, 2002). Effects of transcranial magnetic stimulation known as a treatment for neurological disorders, on motor cortex blood flow and tissue oxygenation have been studied in seven healthy adults during and after the process. Diffused correlations spectroscopy (DCS) and diffused optical spectroscopy (DOS) have been used to monitor the blood flow and hemoglobin concentrations respectively. The results showed an increase in CBF (33 %) on the ipsilateral side and oxygen consumption rate (28 %) in the stimulated region (Mesquita et al., 2013). The role of potassium ions in mediating activity dependent increase in cerebral blood flow was investigated in rat brains by using laser Doppler flowmetry and ion-selective micro-electrodes. Stimulation of parallel and climbing fibers along with KCl microinjections all led to an increase in potassium ion concentrations with subsequent increase of cerebral blood flow. The study concludes that potassium ion concentration increase regulates cerebral blood flow in parallel fiber systems but has lesser consequences in the climbing fiber systems (Caesar et al., 1999).

4.3. Interstitial fluid flow

The flow of ISF in the spaces between and around the cells in the brain parenchyma can occur by the process of molecular diffusion and advective or bulk flow depending on the area. Bulk flow due to hydrostatic or osmotic pressure difference and molecular diffusion of ISF have both been reported in earlier studies. Thus, the proper transport mechanism needs detailed examination under normal and hyperosmolar conditions. In this context, it is relevant to mention the investigation of tissue penetration profiles of a molecule at different time intervals after ventriculocisternal perfusion. Though the diffusion coefficient values of the grey matter remained fairly constant with time that of white matter decreased suggesting bulk flow transport of ISF in those areas. Lastly, 20 % mannitol (1.5–3 g/ Kg) was administered intravenously before 4-h ventriculocisternal perfusion for creating hyperosmolar conditions, which resulted in bulk flow of ISF in grey matter as well. The convection of the ISF in the brain parenchyma can be increased by intracranial perfusions of therapeutic agents known as convection enhanced delivery. It is a modern technique in which a pressure gradient at the tip of a catheter helps in driving the flow of drugs through the brain tissue. This method of drug delivery by increasing the convection of the interstitial fluid has some advantages over other methods. By this process, specific amounts of drugs can be precisely delivered at the required site, bypassing the tight junctions of the blood-brain barrier. Disturbingly, application of convection alone to implanted tumors in mice actually increases invasion of the tumor cells into the surrounding brain parenchyma (Cornelison et al., 2018). Therefore, though this technique is extremely useful for treatment of glioblastoma, AD etc., a more research needs to be done in order to perfect the technique and overcome limitations (Mehta et al., 2017).

Aquaporin-4 (AQP4) is a water channel protein on astrocytic end feet that plays a large role in regulating interstitial fluid flow by regulating water efflux from astrocytes (Nagelhus and Ottersen, 2019). Studies have shown that in AQP4 knockout rats, there is decreased clearance and increased accumulation of ISF in the extracellular space of the caudate nucleus (Teng et al., 2018). AQP4 expression levels vary directly after induction of neurological impairments such as Traumatic Brain injury, hydrocephalus, and Cerebral ischemia, eluding to the transient role AQP4 may have after injury (Hsu et al., 2015).

Manipulation of one compartment of fluid leads to effects on other compartments and thus, dissecting out the individual impacts of these techniques can be difficult and challenging. It also requires knowledge of the proper regions to target within the brain (sources of fluid entry or exit). Recently the meningeal lymphatics followed by the cribriform lymphatics and arachnoid lymphatics have caused neuroscientists and neuro-immunologists to re-evaluate the ability to impact fluid flow in the brain. Since the initial publications on these vessels in 2015 (Louveau et al., 2015), a host of publications have emerged that

are attempting to measure, manipulate, and model these flows (reviewed in (Da Mesquita et al., 2018a, Da Mesquita et al., 2018b)). Primarily, these lymphatics, like lymphatics in the rest of the body, can be targeted through the VEGF Receptor 3 by delivery of its ligand VEGFC. Da Mesquita et al. showed that by either delivery of adenoviruses to transfect meningeal cells to overexpress mVEGFC or through the use of an applied hydrogel which delivered VEGFC over 14 days, aged mice had lessened cognitive deficits and increased CSF flow through the parenchyma and increased drainage to deep cervical nodes (Da Mesquita et al., 2018b). This study highlights the intricate connections between flow compartments, neurological function, and behavior and offers insight into the ability of this ever-present force to affect change in the brain.

5. Conclusion

Fluid flow in the brain is an important element of brain function and defined by elements of the brain structure. Thus far, most studies look at the independent fluid compartments of the brain by focusing on either the CSF, CBF, or ISF, however, we know that these flows are intricately connected. As we gain more precise measurements of these individual components in normal and diseased brains we may be able to better link the compartments in computational models, as is beginning to happen. Additionally, as we grow our hypotheses that govern the role of fluid flow in cellular behaviors, methods to manipulate flow will become more important. However, caution should be used that when increasing fluid in one region (CSF) it is inevitable that other flows will be affected. This includes not only flow rates and pressures, but also the molecular composition of these fluids. Many scientists and researchers think of the CBF, ISF, and CSF as distinctive components that do not mix except in very limited regions, however, because of mass transport and flow within the entire brain they are always linked. Thus, only by better understanding the effects of fluid flow on the cells and tissues of the brain, will we understand the implications of targeting each for therapeutic purposes. To test these, development and use of *in vitro* models is essential for connecting the more global fluid flow changes to microscopic changes to neural function and disease.

Declaration of Competing Interest

None.

Acknowledgement

The authors acknowledge financial support from the National Cancer InstituteR37CA222563.

References

- Abbott, N.J., 2004. Evidence for bulk flow of brain interstitial fluid: significance for physiology and pathology. *Neurochem. Int.* 45, 545–552. <https://doi.org/10.1016/j.neuint.2003.11.006>.
- Absinta, M., Ha, S.-K., Nair, G., Sati, P., Luciano, N.J., Palisoc, M., Louveau, A., Zaghloul, K.A., Pittaluga, S., Kipnis, J., Reich, D.S., 2017. Human and nonhuman primate meninges harbor lymphatic vessels that can be visualized noninvasively by MRI. *Elife* 6. <https://doi.org/10.7554/eLife.29738>.
- Alexandrov, A.V., Bladin, C.F., Norris, J.W., 1994. Intracranial blood flow velocities in acute ischemic stroke. *Stroke*. <https://doi.org/10.1161/01.STR.25.7.1378>.
- Andrews, R.J., Bringas, J.R., Alonzo, G., 1994. Cerebrospinal fluid pH and pCO₂ rapidly follow arterial blood pH and pCO₂ with changes in ventilation. *Neurosurgery* 34, 466–470. <https://doi.org/10.1227/00006123-199403000-00012>.
- Arbel-Ornath, M., Hudry, E., Eikermann-Haerter, K., Hou, S., Gregory, J.L., Zhao, L., Betensky, R.A., Frosch, M.P., Greenberg, S.M., Bacskai, B.J., 2013. Interstitial fluid drainage is impaired in ischemic stroke and Alzheimer's disease mouse models. *Acta Neuropathol.* 126, 353–364. <https://doi.org/10.1007/s00401-013-1145-2>.
- Aspelund, A., Antila, S., Proulx, S.T., Karlén, T.V., Karaman, S., Detmar, M., Wiig, H., Alitalo, K., 2015. A dural lymphatic vascular system that drains brain interstitial fluid and macromolecules. *J. Exp. Med.* 212, 991–999. <https://doi.org/10.1084/jem.20142290>.
- Baser, P.J., n.d. Interstitial Pressure, Volume, and Flow during Infusion into Brain Tissue.
- Basser, P.J., Mattiello, J., LeBihan, D., 1994. MR diffusion tensor spectroscopy and imaging. *Biophys. J.* [https://doi.org/10.1016/S0006-3495\(94\)80775-1](https://doi.org/10.1016/S0006-3495(94)80775-1).
- Battal, B., Kocaoglu, M., Bulakbasi, N., Husmen, G., Tuba Sanal, H., Tayfun, C., 2011. Cerebrospinal fluid flow imaging by using phase-contrast MR technique. *Br. J. Radiol.* <https://doi.org/10.1259/bjr/66206791>.
- Baxter, L.T., Jain, R.K., 1989. Transport of fluid and macromolecules in tumors. I. Role of interstitial pressure and convection. *Microvasc. Res.* 37, 77–104. [https://doi.org/10.1016/0026-2862\(89\)90074-5](https://doi.org/10.1016/0026-2862(89)90074-5).
- Bedussi, B., Almasian, M., de Vos, J., VanBavel, E., Bakker, E.N.T.P., 2018. Paravascular spaces at the brain surface: Low resistance pathways for cerebrospinal fluid flow. *J. Cereb. Blood Flow Metab.* 38, 719–726. <https://doi.org/10.1177/0271678X17737984>.
- Bedussi, B., van Lier, M.G.J.T.B., Bartstra, J.W., de Vos, J., Siebes, M., VanBavel, E., Bakker, E.N.T.P., 2015. Clearance from the mouse brain by convection of interstitial fluid towards the ventricular system. *Fluids Barriers CNS* 12, 1–13. <https://doi.org/10.1186/s12987-015-0019-5>.
- Begley, D.J., 2004. Delivery of therapeutic agents to the central nervous system: the problems and the possibilities. *Pharmacol. Ther.* <https://doi.org/10.1016/j.pharmthera.2004.08.001>.
- Berger, A., 2002. How does it work?: magnetic resonance imaging. *BMJ*. <https://doi.org/10.1136/bmj.324.7328.35>.
- Bloomfield, I.G., Johnston, I.H., Bilston, L.E., 1998. Effects of proteins, blood cells and glucose on the viscosity of cerebrospinal fluid. *Pediatr. Neurosurg.* 28, 246–251. <https://doi.org/10.1159/000028659>.
- Bonte, F.J., Harris, T.S., Hyman, L.S., Bigio, E.H., White, C.L., 2006. Tc-99m HMPAO SPECT in the differential diagnosis of the dementias with histopathologic confirmation. *Clin. Nucl. Med.* <https://doi.org/10.1097/01.rlu.0000222736.81365.63>.
- Booth, R., Kim, H., 2012. Characterization of a microfluidic in vitro model of the blood-brain barrier (uBBB). *Lab Chip* 12, 1784–1792. <https://doi.org/10.1039/c2lc40094d>.
- Boucher, Y., Baxter, L.T., Jain, R.K., 1990. Interstitial pressure gradients in tissue-isolated and subcutaneous tumors: implications for therapy. *Cancer Res.* 50, 4478–4484.
- Boucher, Y., Salehi, H., Witwer, B., Harsh, G.R., Jain, R.K., 1997. Interstitial fluid pressure in intracranial tumours in patients and in rodents. *Br. J. Cancer* 75, 829–836. <https://doi.org/10.1038/bjc.1997.148>.
- Boye, D., Montali, M., Miller, N.R., Pircher, A., Gruber, P., Killer, H.E., Remonda, L., Berberat, J., 2018. Flow dynamics of cerebrospinal fluid between the intracranial cavity and the subarachnoid space of the optic nerve measured with a diffusion magnetic resonance imaging sequence in patients with normal tension glaucoma. *Clin. Exp. Ophthalmol.* 46, 511–518. <https://doi.org/10.1111/ceo.13116>.
- Brooks, D.J., 2005. Positron emission tomography and single-photon emission computed tomography in central nervous system drug development. *NeuroRx*. <https://doi.org/10.1602/neuroRx.2.2.226>.
- Caesar, K., Akgören, N., Mathiesen, C., Lauritzen, M., 1999. Modification of activity-dependent increases in cerebellar blood flow by extracellular potassium in anaesthetized rats. *J. Physiol.* 520, 281–292. <https://doi.org/10.1111/j.1469-7793.1999.00281.x>.
- Chin, J.H., 2014. Tuberculous meningitis: diagnostic and therapeutic challenges. *Neurol. Clin. Pract.* <https://doi.org/10.1212/CPJ.0000000000000023>.
- Choi, Y.J., Chae, S., Kim, J.H., Barald, K.F., Park, J.Y., Lee, S.H., 2013. Neurotoxic amyloid beta oligomeric assemblies recreated in microfluidic platform with interstitial level of slow flow. *Sci. Rep.* 3, 1–7. <https://doi.org/10.1038/srep01921>.
- Cornelison, R.C., Brennan, C.E., Kingsmore, K.M., Munson, J.M., 2018. Convective forces increase CXCR4-dependent glioblastoma cell invasion in GL261 murine model. *Sci. Rep.* 1–11. <https://doi.org/10.1038/s41598-018-35141-9>.
- Crawford, F., Suo, Z., Fang, C., Sawar, A., George, S.U., Arendash, G., Mullan, M., 1997. The vasoactivity of Aβ peptides. *Ann. N. Y. Acad. Sci.* <https://doi.org/10.1111/j.1749-6632.1997.tb48459.x>.
- Cserr, H.F., 1988. Role of secretion and bulk flow of brain interstitial fluid in brain volume regulation. *Ann. N. Y. Acad. Sci.* 529, 9–20. <https://doi.org/10.1111/j.1749-6632.1988.tb51415.x>.
- Cutnell, J.D., Johnson, K.W., 1998. *Physics*. Wiley.
- Da Mesquita, S., Fu, Z., Kipnis, J., 2018a. Perspective the meningeal lymphatic system: a new player in neurophysiology. *Neuron* 100, 375–388. <https://doi.org/10.1016/j.neuron.2018.09.022>.
- Da Mesquita, S., Louveau, A., Vaccari, A., Smirnov, I., Cornelison, R.C., Kingsmore, K.M., Contarino, C., Onengut-Gumuscu, S., Farber, E., Raper, D., Viar, K.E., Powell, R.D., Baker, W., Dabhi, N., Cao, R., Hu, S., Rich, S., Munson, J.M., Lopes, M.B., Overall, C.C., Acton, S.T., Kipnis, J., 2018b. Functional aspects of meningeal lymphatics in ageing and Alzheimer's disease. *Nature* 560, 185–191.
- Dai, W., Astary, G.W., Kasinadhuni, A.K., Carney, P.R., Mareci, T.H., Sarntinoranont, M., 2016. Voxelized model of brain infusion that accounts for small feature fissures: comparison with magnetic resonance tracer studies. *J. Biomech. Eng.* 138, 051007. <https://doi.org/10.1115/1.4032626>.
- de Eulate, R.G., Goñi, I., Galiano, A., Vidorreta, M., Recio, M., Riverol, M., Zubieta, J.L., Fernández-Seara, M.A., 2017. Reduced cerebral blood flow in mild cognitive impairment assessed using phase-contrast MRI. *J. Alzheimers Dis.* 58, 585–595. <https://doi.org/10.3233/JAD-161222>.
- Devous, M.D., 2005. Single-photon emission computed tomography in neurotherapeutics. *NeuroRx*. <https://doi.org/10.1602/neuroRx.2.2.237>.
- Di Terlizzi, R., Platt, S., 2006. The function, composition and analysis of cerebrospinal fluid in companion animals: part I - function and composition. *Vet. J.* 172, 422–431. <https://doi.org/10.1016/j.tvjl.2005.07.021>.
- Doepf, F., Schreiber, S.J., von Münster, T., Rademacher, J., Klingebiel, R., Valdueza, J.M., 2004. How does the blood leave the brain? A systematic ultrasound analysis of cerebral venous drainage patterns. *Neuroradiology* 46, 565–570. <https://doi.org/10.1007/s00234-004-1213-3>.
- Dreha-Kulaczewski, S., Joseph, A.A., Merboldt, K.-D., Ludwig, H.-C., Gartner, J., Frahm,

- J., 2015. Inspiration is the major regulator of human CSF flow. *J. Neurosci.* 35, 2485–2491. <https://doi.org/10.1523/JNEUROSCI.3246-14.2015>.
- Ehlers, W., Wagner, A., 2015. Multi-component modelling of human brain tissue: a contribution to the constitutive and computational description of deformation, flow and diffusion processes with application to the invasive drug-delivery problem. *Comput. Methods Biomech. Biomed. Eng.* 18, 861–879. <https://doi.org/10.1080/10255842.2013.853754>.
- Eide, P.K., Vatnehol, S.A.S., Emblem, K.E., Ringstad, G., 2018. Magnetic resonance imaging provides evidence of glymphatic drainage from human brain to cervical lymph nodes. *Sci. Rep.* 8, 1–10. <https://doi.org/10.1038/s41598-018-25666-4>.
- Fantini, S., Sassaroli, A., Tgavalekos, K.T., Kornbluth, J., 2016. Cerebral blood flow and autoregulation: current measurement techniques and prospects for noninvasive optical methods. *Neurophotonics* 3, 031411. <https://doi.org/10.1117/1.NPh.3.3.031411>.
- Faubel, R., Westendorf, C., Bodenschatz, E., Eichele, G., 2016. Cilia-based flow network in the brain ventricles. *Science* 353(6353), 176–178. <https://doi.org/10.1126/science.1255842>.
- Feng, T., Iliff, J.J., Nedergaard, M., Lee, H., Benveniste, H., Logan, J., Yu, M., 2013. Brain-wide pathway for waste clearance captured by contrast-enhanced MRI. *J. Clin. Invest.* 123, 1299–1309. <https://doi.org/10.1172/jci67677>.
- Ferrandez, A., David, T., Brown, M.D., 2002. Numerical models of auto-regulation and blood flow in the cerebral circulation. *Comput. Methods Biomech. Biomed. Eng.* 5, 7–20. <https://doi.org/10.1080/10255840290032171>.
- Frackowiak, R.S.J., Lenzi, G.L., Jones, T., Heather, J.D., 1980. Quantitative measurement of regional cerebral blood flow and oxygen metabolism in man using ¹⁵O and positron emission tomography: theory, procedure, and normal values. *J. Comput. Assist. Tomogr.* <https://doi.org/10.1097/00004728-198012000-00001>.
- Gabriel, E.M., Fisher, D.T., Evans, S., Takabe, K., Skitzki, J.J., 2018. Intravital microscopy in the study of the tumor microenvironment: from bench to human application. *Oncotarget*. <https://doi.org/10.18632/oncotarget.24957>.
- Gadda, G., Taibi, A., Sisini, F., Gambaccini, M., Zamboni, P., Ursino, M., 2015. A new hemodynamic model for the study of cerebral venous outflow. *Am. J. Physiol. Circ. Physiol.* 308, H217–H231. <https://doi.org/10.1152/ajpheart.00469.2014>.
- Geer, C.P., Grossman, S.A., 1997. Interstitial fluid flow along white matter tracts: a potentially important mechanism for the dissemination of primary brain tumors. *J. Neuro-Oncol.*
- Grinberg, Leopold, Anor, T., Cheever, E., Madsen, J.R., Karniadakis, G.E., 2009a. Simulation of the human intracranial arterial tree. *Philos. Trans. R. Soc. A Math. Phys. Eng. Sci.* 367, 2371–2386. <https://doi.org/10.1098/rsta.2008.0307>.
- Grinberg, L., Anor, T., Madsen, J.R., Yakhot, A., Karniadakis, G.E., 2009b. Large-scale simulation of the human arterial tree. *Clin. Exp. Pharmacol. Physiol.* 36, 194–205. <https://doi.org/10.1111/j.1440-1681.2008.05010.x>.
- Grzybowski, D.M., Holman, D.W., Katz, S.E., Lubow, M., 2006. In vitro model of cerebrospinal fluid outflow through human arachnoid granulations. *Investig. Ophthalmol. Vis. Sci.* 47, 3664–3672. <https://doi.org/10.1167/iov.05-0929>.
- Guan, X., Wang, W., Wang, A., Teng, Z., Han, H., 2017. Brain interstitial fluid drainage alterations in glioma-bearing rats. *Aging Dis.* 9, 228. <https://doi.org/10.14336/ad.2017.0415>.
- Gupta, S., Soellinger, M., Boesiger, P., Poulikakos, D., Kurtcuoglu, V., 2009. Three-dimensional computational modeling of subject-specific cerebrospinal fluid flow in the subarachnoid space. *J. Biomech. Eng.* 131, 021010. <https://doi.org/10.1115/1.3005171>.
- Gupta, S., Soellinger, M., Grzybowski, D.M., Boesiger, P., Biddiscombe, J., Poulikakos, D., Kurtcuoglu, V., 2010. Cerebrospinal fluid dynamics in the human cranial subarachnoid space: an overlooked mediator of cerebral disease. *I. Comput. Model. J. R. Soc. Interface* 7, 1195–1204. <https://doi.org/10.1098/rsif.2010.0033>.
- Hadjihambi, A., Harrison, I.F., Costas-Rodríguez, M., Vanhaecke, F., Arias, N., Gallego-Durán, R., Mastitskaya, S., Hosford, P.S., Olde Damink, S.W.M., Davies, N., Habtesion, A., Lythgoe, M.F., Gourine, A.V., Jalan, R., 2019. Impaired brain glymphatic flow in experimental hepatic encephalopathy. *J. Hepatol.* 70, 40–49. <https://doi.org/10.1016/j.jhep.2018.08.021>.
- Han, H.B., Li, K., Yan, J.H., Zhu, K., Fu, Y., 2012. An in vivo study with an MRI tracer method reveals the biophysical properties of interstitial fluid in the rat brain. *Sci. China Life Sci.* 55, 782–787. <https://doi.org/10.1007/s11427-012-4361-4>.
- Harrison, I.F., Siow, B.A., Akilo, A.B., Evans, P., Ismail, O., Ohene, Y., Nahavandi, P., Thomas, D.L., Lythgoe, M.F., 2018. Non-invasive assessment of glymphatic inflow: measurement of perivascular fluid movement using diffusion tensor MRI. *Elife* 7, 1–14. <https://doi.org/10.1101/281311>.
- Helminger, G., Yuan, F., Dellian, M., Jain, R.K., 1997. Interstitial pH and pO₂ gradients in solid tumors in vivo: High-resolution measurements reveal a lack of correlation. *Nat. Med.* 3, 177–182. <https://doi.org/10.1038/nm0297-177>.
- Herscovitch, P., Markham, J., Raichle, M.E., 1983. Brain blood flow measured with intracranial H₂(15)O. I. Theory and error analysis. *J. Nucl. Med.* 24, 782–789.
- Hsu, Y., Tran, M., Linninger, A.A., 2015. Dynamic Regulation of aquaporin-4 Water Channels in Neurological Disorders. pp. 401–421. <https://doi.org/10.3325/cmj.2015.56.401>.
- Iliff, J.J., Wang, M., Liao, Y., Plogg, B., Peng, W., Gundersen, G., Benveniste, H., Vates, G.E., Deane, R., Goldman, S., Nagelhus, E., Nedergaard, M., 2012. A paravascular pathway facilitates CSF flow through the brain parenchyma and the clearance of interstitial solutes, including amyloid. *Sci. Transl. Med.* 4, 147ra111–147ra111. <https://doi.org/10.1126/scitranslmed.3003748>.
- Iliff, J.J., Wang, M., Zeppenfeld, D.M., Venkataraman, A., Plog, B.A., Liao, Y., Deane, R., Nedergaard, M., 2013. Cerebral arterial pulsation drives paravascular CSF-interstitial fluid exchange in the murine brain. *J. Neurosci.* 33, 18190–18199. <https://doi.org/10.1523/jneurosci.1592-13.2013>.
- Ivanov, K.P., Kalinina, M.K., Levkovich, Y.I., 1981. Blood flow velocity in capillaries of brain and muscles and its physiological significance. *Microvasc. Res.* 22, 143–155. [https://doi.org/10.1016/0026-2862\(81\)90084-4](https://doi.org/10.1016/0026-2862(81)90084-4).
- Kim, J.H., Astary, G.W., Kantorovich, S., Mareci, T.H., Carney, P.R., Sarntinoranont, M., 2012. Voxelized computational model for convection-enhanced delivery in the rat ventral hippocampus: comparison with in vivo MR experimental studies. *Ann. Biomed. Eng.* 40, 2043–2058. <https://doi.org/10.1007/s10439-012-0566-8>.
- Kimbrough, I.F., Robel, S., Roberson, E.D., Sontheimer, H., 2015. Vascular amyloidosis impairs the gliovascular unit in a mouse model of Alzheimer's disease. *Brain* 138, 3716–3733. <https://doi.org/10.1093/brain/awv327>.
- Kingsmore, K.M., Logsdon, D.K., Floyd, D.H., Peirce, S.M., Purwo, B.W., Munson, J.M., 2016. Interstitial flow differentially increases patient-derived glioblastoma stem cell invasion via CXCR4, CXCL12, and CD44-mediated mechanisms. *Integr. Biol.* 4, 127ra36. <https://doi.org/10.1039/C6IB00167J>.
- Kingsmore, K.M., Vaccari, A., Abler, D., Cui, S.X., Epstein, F.H., Rockne, R.C., Acton, S.T., Munson, J.M., 2018. MRI analysis to map interstitial flow in the brain tumor microenvironment. *APL Bioeng.* 2, 031905. <https://doi.org/10.1063/1.5023503>.
- Klarica, M., Rados, M., Draganic, P., Erceg, G., Oreskovic, D., Maraković, J., Bulat, M., 2006. Effect of head position on cerebrospinal fluid pressure in cats: comparison with artificial model. *Croat. Med. J.*
- Kurtcuoglu, V., Poulikakos, D., Ventikos, Y., 2005. Computational modeling of the mechanical behavior of the cerebrospinal fluid system. *J. Biomech. Eng.* 127, 264. <https://doi.org/10.1115/1.1865191>.
- Kurtcuoglu, V., Soellinger, M., Summers, P., Boomsma, K., Poulikakos, D., Boesiger, P., Ventikos, Y., 2007. Computational investigation of subject-specific cerebrospinal fluid flow in the third ventricle and aqueduct of Sylvius. *J. Biomech.* 40, 1235–1245. <https://doi.org/10.1016/j.jbiomech.2006.05.031>.
- Lameka, K., Farwell, M.D., Ichise, M., 2016. Positron Emission Tomography. pp. 209–227. <https://doi.org/10.1016/B978-0-444-53485-9.00011-8>.
- Lee, H., Mortensen, K., Sanggaard, S., Koch, P., Brunner, H., Quistorff, B., Nedergaard, M., Benveniste, H., 2018. Quantitative Gd-DOTA uptake from cerebrospinal fluid into rat brain using 3D VFA-SPGR at 9.4T. *Magn. Reson. Med.* 79, 1568–1578. <https://doi.org/10.1002/mrm.26779>.
- Lei, Y., Han, H., Yuan, F., Javed, A., Zhao, Y., 2017. The brain interstitial system: anatomy, modeling, in vivo measurement, and applications. *Prog. Neurobiol.* 157, 230–246. <https://doi.org/10.1016/j.pneurobio.2015.12.007>.
- Levin, E., Muravchick, S., Gold, M.I., 1981. Density of normal human cerebrospinal fluid and tetraacetic solutions. *Anesth. Analg.* 60, 814–817.
- Liang, X., Zou, Q., He, Y., Yang, Y., 2013. Coupling of functional connectivity and regional cerebral blood flow reveals a physiological basis for network hubs of the human brain. *Proc. Natl. Acad. Sci.* 110, 1929–1934. <https://doi.org/10.1073/pnas.1214900110>.
- Lindström, E.K., Ringstad, G., Mardal, K.A., Eide, P.K., 2018. Cerebrospinal fluid volumetric net flow rate and direction in idiopathic normal pressure hydrocephalus. *Neuroimage Clin.* 20, 731–741. <https://doi.org/10.1016/j.nicl.2018.09.006>.
- Linninger, A.A., Xenos, M., Sweetman, B., Ponskhe, S., Guo, X., Penn, R., 2009. A mathematical model of blood, cerebrospinal fluid and brain dynamics. *J. Math. Biol.* 59, 729–759. <https://doi.org/10.1007/s00285-009-0250-2>.
- Linninger, A.A., Xenos, M., Zhu, D.C., Somayaji, M.B.R., Kondapalli, S., Penn, R.D., 2007. Cerebrospinal fluid flow in the normal and hydrocephalic human brain. *IEEE Trans. Biomed. Eng.* 54, 291–302. <https://doi.org/10.1109/TBME.2006.886853>.
- Lotz, J., Meier, C., Leppert, A., Galanski, M., 2002. Cardiovascular flow measurement with phase-contrast MR imaging: basic facts and implementation. *RadioGraphics*. <https://doi.org/10.1148/radiographics.22.3.g02mal1651>.
- Louveau, A., Smirnov, I., Keyes, T.J., Eccles, J.D., Rouhani, S.J., Peske, J.D., Derecki, N.C., Castle, D., Mandell, J.W., Lee, K.S., Harris, T.H., Kipnis, J., 2015. Structural and functional features of central nervous system lymphatic vessels. *Nature* 523, 337–341. <https://doi.org/10.1038/nature14432>.
- Lysakowski, C., Walder, B., Costanza, M.C., Tramèr, M.R., 2001. Transcranial Doppler versus angiography in patients with vasospasm due to a ruptured cerebral aneurysm: a systematic review. *Stroke* 32, 2292–2298. <https://doi.org/10.1161/hs1001.097108>.
- Mehta, A.M., Sonabend, A.M., Bruce, J.N., 2017. Convection-enhanced delivery. *Neurotherapeutics* 14, 358–371. <https://doi.org/10.1007/s13311-017-0520-4>.
- Mesquita, R.C., Buckley, E.M., Kim, M.N., Yodh, A.G., Faseyitan, O.K., Thomas, A., Greenberg, J.H., Detre, J.A., Hamilton, R.H., Turkeltaub, P.E., Durduran, T., 2013. Blood flow and oxygenation changes due to low-frequency repetitive transcranial magnetic stimulation of the cerebral cortex. *J. Biomed. Opt.* 18. <https://doi.org/10.1117/1.JBO.18.6.067006>.
- Mestre, H., Tithof, J., Du, T., Song, W., Peng, W., Sweeney, A.M., Olveda, G., Thomas, J.H., Nedergaard, M., Kelley, D.H., 2018a. Flow of cerebrospinal fluid is driven by arterial pulsations and is reduced in hypertension. *Nat. Commun.* 9, 4878. <https://doi.org/10.1038/s41467-018-07318-3>.
- Miller, B., Nagy, D., Finlay, B.L., Chance, B., Kobayashi, A., Nioka, S., 1993. Consequences of reduced cerebral blood flow in brain development. I. Gross morphology, histology, and callosal connectivity. *Exp. Neurol.* <https://doi.org/10.1006/exnr.1993.1203>.
- Miracourt, O., Salmon, S., Szopos, M., Thiriet, M., Miracourt, O., Salmon, S., Szopos, M., Thiriet, M., 2016. Blood Flow in the Cerebral Venous System: Modeling and Simulation to Cite This Version: HAL id: hal-01384285.
- Miyani, J.A., Zendah, M., Mashayekhi, F., Owen-Lynch, P.J., 2006. Cerebrospinal fluid supports viability and proliferation of cortical cells in vitro, mirroring in vivo development. *Cerebrospinal Fluid Res.* 3, 1–7. <https://doi.org/10.1186/1743-8454-3-2>.
- Munson, J.M., Bellamkonda, R.V., Swartz, M.A., 2013. Interstitial flow in a 3d microenvironment increases glioma invasion by a cxcr4-dependent mechanism. *Cancer Res.* 73, 1536–1546. <https://doi.org/10.1158/0008-5472.CAN-12-2838>.
- Nagelhus, E.A., Ottersen, O.P., 2019. Physiological Roles of AQUAPORIN-4 Regulation Water and Waste Clearance Sensory Systems. pp. 1543–1562. <https://doi.org/10.1002/wat.1200>.

- 1152/physrev.00011.2013.
- Nassar, B.R., Lippa, C.F., 2016. Idiopathic normal pressure hydrocephalus: a review for general practitioners. *Gerontol. Geriatr. Med.* <https://doi.org/10.1177/2333721416643702>.
- Naylor, G.L., Firmin, D.N., Longmore, D.B., 1986. Blood flow imaging by cine magnetic resonance. *J. Comput. Assist. Tomogr.* 10, 715–722.
- Ogoh, S., 2017. Relationship between cognitive function and regulation of cerebral blood flow. *J. Physiol. Sci.* <https://doi.org/10.1007/s12576-017-0525-0>.
- Owler, B.K., Pena, A., Momjian, S., Czosnyka, Z., Czosnyka, M., Harris, N.G., Smielewski, P., Fryer, T., Donvan, T., Carpenter, A., Pickard, J.D., 2004. Changes in cerebral blood flow during cerebrospinal fluid pressure manipulation in patients with normal pressure hydrocephalus: a methodological study. *J. Cereb. Blood Flow Metab.* 24, 579–587. <https://doi.org/10.1097/00004647-200405000-00012>.
- Park, J., Lee, B.K., Jeong, G.S., Hyun, J.K., Lee, C.J., Lee, S.H., 2015a. Three-dimensional brain-on-a-chip with an interstitial level of flow and its application as an in vitro model of Alzheimer's disease. *Lab Chip* 15, 141–150. <https://doi.org/10.1039/c4lc00962b>.
- Paterson, R.W., Gabelle, A., Lucey, B.P., Barthélemy, N.R., Leckey, C.A., Hirtz, C., Lehmann, S., Sato, C., Patterson, B.W., West, T., Yarasheski, K., Rohrer, J.D., Wildburger, N.C., Schott, J.M., Karch, C.M., Wray, S., Miller, T.M., Elbert, D.L., Zetterberg, H., Fox, N.C., Bateman, R.J., 2019. SILK studies — capturing the turnover of proteins linked to neurodegenerative diseases. *Nat. Rev. Neurol.* <https://doi.org/10.1038/s41582-019-0222-0>.
- Pelc, N.J., Herfkens, R.J., Shimakawa, A., Enzmann, D.R., 1991. Phase contrast cine magnetic resonance imaging. *Magn. Reson. Q.*
- Perdikaris, P., Grinberg, L., Karniadakis, G.E., 2016. Multiscale modeling and simulation of brain blood flow. *Phys. Fluids* 28. <https://doi.org/10.1063/1.4941315>.
- Perlmutter, J.S., 2002. Blood flow responses to deep brain stimulation of thalamus. *Neurology* 58, 1388–1394. <https://doi.org/10.1212/WNL.58.9.1388>.
- Pullen, R.G., DePasquale, M., Cserr, H.F., 2017. Bulk flow of cerebrospinal fluid into brain in response to acute hyperosmolality. *Am. J. Physiol. Physiol.* 253, F538–F545. <https://doi.org/10.1152/ajprenal.1987.253.3.f538>.
- Qazi, H., Palomino, R., Shi, Z.D., Munn, L.L.L., Tarbell, J.M.J.M., 2013. Cancer cell glyocalyx mediates mechanotransduction and flow-regulated invasion. *Integr. Biol. (United Kingdom)* 5, 1334–1343. <https://doi.org/10.1039/c3ib40057c>.
- Quencer, R.M., Donovan Post, M.J., Hinks, R.S., 1990. Cine MR in the evaluation of normal and abnormal CSF flow: intracranial and intraspinal studies. *Neuroradiology* 32, 371–391. <https://doi.org/10.1007/BF00588471>.
- Raghavan, R., Brady, M., 2011. Predictive models for pressure-driven fluid infusions into brain parenchyma. *Phys. Med. Biol.* 56, 6179–6204. <https://doi.org/10.1088/0031-9155/56/19/003>.
- Rambani, K., Vukasinovic, J., Glezer, A., Potter, S.M., 2009. Culturing thick brain slices: an interstitial 3D microperfusion system for enhanced viability. *J. Neurosci. Methods* 180, 243–254. <https://doi.org/10.1016/j.jneumeth.2009.03.016>.
- Rennels, M.L., Blaumanis, O.R., Grady, P.A., 1990. Rapid solute transport throughout the brain via paravascular fluid pathways. *Adv. Neurol.* 52, 431–439.
- Rey, J., Sarntinoranont, M., 2018. Pulsatile flow drivers in brain parenchyma and perivascular spaces: a resistance network model study. *Fluids Barriers CNS* 15, 1–11. <https://doi.org/10.1186/s12987-018-0105-6>.
- Sarkar, S., Ghosh, S., Ghosh, S.K., Collier, A., 2007. Role of transcranial Doppler ultrasonography in stroke. *Postgrad. Med. J.* <https://doi.org/10.1136/pgmj.2007.058602>.
- Sato, K., Sadamoto, T., 2010. Different blood flow responses to dynamic exercise between internal carotid and vertebral arteries in women. *J. Appl. Physiol.* 109, 864–869. <https://doi.org/10.1152/jappphysiol.01359.2009>.
- Sawamoto, K., Wichterle, H., Gonzalez-Perez, O., Cholfin, J.A., Yamada, M., Spassky, N., Murcia, N.S., Garcia-Verdugo, J.M., Marin, O., Rubenstein, J.L.R., Tessier-Lavigne, M., Okano, H., Alvarez-Buylla, A., 2006. New neurons follow the flow of cerebrospinal fluid in the adult brain. *Science (80-)* 311, 629–632.
- Shimizu, H., Inoue, T., Fujimura, M., Saito, A., Tominaga, T., 2011. Cerebral blood flow after surgery for unruptured cerebral aneurysms: Effects of surgical manipulation and irrigation fluid. *Neurosurgery* 69, 677–688. <https://doi.org/10.1227/NEU.0b013e3182195509>.
- Simon, M.J., Iliff, J.J., 2016. Regulation of cerebrospinal fluid (CSF) flow in neurodegenerative, neurovascular and neuroinflammatory disease. *Biochim. Biophys. Acta - Mol. Basis Dis.* <https://doi.org/10.1016/j.bbadis.2015.10.014>.
- Smitha, K.A., Akhil Raja, K., Arun, K.M., Rajesh, P.G., Thomas, B., Kapilamoorthy, T.R., Kesavadas, C., 2017. Resting state fMRI: a review on methods in resting state connectivity analysis and resting state networks. *Neuroradiol. J.* <https://doi.org/10.1177/1971400917697342>.
- Steinman, D.A., Milner, J.S., Norley, C.J., Lownie, S.P., Holdsworth, D.W., 2003. Image-Based Computational Simulation. pdf. pp. 559–566. <https://doi.org/10.3174/ajnr.A2121>.
- Stephan, K.E., Friston, K.J., 2010. Functional connectivity. *Encycl. Neurosci.* <https://doi.org/10.1016/B978-008045046-9.00308-9>.
- Sweetman, B., Xenos, M., Zitella, L., Linninger, A.A., 2011. Three-dimensional computational prediction of cerebrospinal fluid flow in the human brain. *Comput. Biol. Med.* 41, 67–75. <https://doi.org/10.1016/j.compbiomed.2010.12.001>.
- Tanner, J.E., Stejskal, E.O., 1968. Restricted self-diffusion of protons in colloidal systems by the pulsed-gradient, spin-echo method. *J. Chem. Phys.* <https://doi.org/10.1063/1.1670306>.
- Tate, K.M., Munson, J.M., 2019. Assessing drug response in engineered neural micro-environment. *Brain Res. Bull.* 150, 21–34.
- Teng, Z., Wang, A., Wang, P., Wang, R., Wang, W., Han, H., 2018. The effect of aquaporin-4 knockout on interstitial fluid flow and the structure of the extracellular space in the deep brain. *Aging Dis.* 9, 808–816.
- Tomiya, Y., Brian, J.E., Todd, M.M., 2000. Plasma viscosity and cerebral blood flow. *Am. J. Physiol. - Hear. Circ. Physiol.* 279. <https://doi.org/10.1152/ajpheart.2000.279.4.h1949>.
- Tully, B., Ventikos, Y., 2011. Cerebral water transport using multiple-network poroelastic theory: application to normal pressure hydrocephalus. *J. Fluid Mech.* 667, 188–215. <https://doi.org/10.1017/S0022112010004428>.
- Ursino, M., Lodi, C.A., 2017. A simple mathematical model of the interaction between intracranial pressure and cerebral hemodynamics. *J. Appl. Physiol.* 82, 1256–1269. <https://doi.org/10.1152/jappphysiol.1997.82.4.1256>.
- Veall, N., Mallett, B.L., 1965. The partition of trace amounts of xenon between human blood and brain tissues at 37°C. *Phys. Med. Biol.* <https://doi.org/10.1088/0031-9155/10/3/306>.
- Voipio, J., Ballanyi, K., 1997. Interstitial P(CO₂) and pH, and their role as chemostimulants in the isolated respiratory network of neonatal rats. *J. Physiol.* 499, 527–542. <https://doi.org/10.1113/jphysiol.1997.sp021946>.
- Wählin, A., Ambarki, K., Hauksson, J., Birgander, R., Malm, J., Eklund, A., 2012. Phase contrast MRI Quantification of pulsatile volumes of brain arteries, veins, and cerebrospinal fluids compartments: repeatability and physiological interactions. *J. Magn. Reson. Imaging.* <https://doi.org/10.1002/jmri.23527>.
- Wang, Y.I., Erbil Abaci, H., Shuler Nancy, E.M.L., 2017a. Microfluidic blood-brain barrier model provides in vivo-like barrier properties for drug permeability screening: Microfluidic blood-brain barrier model provides in vivo-like barrier properties for drug permeability screening. *Biotechnol. Bioeng.* 114, 184–194. <https://doi.org/10.1002/bit.26045/abstract>.
- Wu, Y., Agarwal, S., Jones, C.K., Webb, A.G., van Zijl, P.C.M., Hua, J., Pillai, J.J., 2016. Measurement of arteriolar blood volume in brain tumors using MRI without exogenous contrast agent administration at 7T. *J. Magn. Reson. Imaging* 44, 1244–1255. <https://doi.org/10.1002/jmri.25248>.
- Yao, W., Li, Y., Ding, G., 2012. Interstitial fluid flow: The mechanical environment of cells and foundation of meridians. Evidence-based Complement. Altern. Med. 2012. <https://doi.org/10.1155/2012/853516>.
- Zaharchuk, G., Martin, A.J., Rosenthal, G., Manley, G.T., Dillon, W.P., 2005. Measurement of cerebrospinal fluid oxygen partial pressure in humans using MRI. *Magn. Reson. Med.* 54, 113–121. <https://doi.org/10.1002/mrm.20546>.
- Zhu, D.C., Xenos, M., Linninger, A.A., Penn, R.D., 2006. Dynamics of lateral ventricle and cerebrospinal fluid in normal and hydrocephalic brains. *J. Magn. Reson. Imaging* 24, 756–770. <https://doi.org/10.1002/jmri.20679>.